Physics Letters B 751 (2015) 311–315

Contents lists available at ScienceDirect

Physics Letters B

www.elsevier.com/locate/physletb

The first science result with the JENSA gas-jet target: Confirmation and study of a strong subthreshold $^{18}F(p,\alpha)^{15}O$ resonance

D.W. Bardayan [a,b,*], K.A. Chipps [b,c,d], S. Ahn [c,e], J.C. Blackmon [f], R.J. deBoer [a], U. Greife [d], K.L. Jones [c], A. Kontos [e], R.L. Kozub [g], L. Linhardt [f], B. Manning [h], M. Matoš [b,c], P.D. O'Malley [a], S. Ota [h], S.D. Pain [b], W.A. Peters [b,c], S.T. Pittman [b,c], A. Sachs [c], K.T. Schmitt [b,c], M.S. Smith [b], P. Thompson [c]

[a] Dept. of Physics, University of Notre Dame, Notre Dame, IN 46556, USA
[b] Physics Division, Oak Ridge National Laboratory, Oak Ridge, TN 37831, USA
[c] Dept. of Physics and Astronomy, University of Tennessee, Knoxville, TN 37996, USA
[d] Physics Dept., Colorado School of Mines, Golden, CO 80401, USA
[e] National Superconducting Cyclotron Laboratory, East Lansing, MI 48824, USA
[f] Dept. of Physics and Astronomy, Louisiana State University, Baton Rouge, LA 70803, USA
[g] Physics Dept., Tennessee Technological University, Cookeville, TN 38505, USA
[h] Dept. of Physics and Astronomy, Rutgers University, Piscataway, NJ 08854, USA

ARTICLE INFO

Article history:
Received 15 July 2015
Received in revised form 9 October 2015
Accepted 26 October 2015
Available online 28 October 2015
Editor: D.F. Geesaman

Keywords:
Novae
Nucleosynthesis
Nuclear
Reactions

ABSTRACT

The astrophysical $^{18}F(p,\alpha)^{15}O$ rate determines, in large part, the extent to which the observable radioisotope ^{18}F is produced in novae. This rate, however, has been extremely uncertain owing to the unknown properties of a strong subthreshold resonance and its possible interference with higher-lying resonances. The new Jet Experiments in Nuclear Structure and Astrophysics (JENSA) gas-jet target has been used for the first time to determine the spin of this important resonance and significantly reduce uncertainties in the $^{18}F(p,\alpha)^{15}O$ rate.

Novae are some of the most energetic and frequent astrophysical explosions in the Universe. Approximately 30 occur each year in the Milky Way galaxy with each releasing $\sim 10^{45}$ ergs of energy [1]. Novae occur in binary systems of stars when accretion of hydrogen-rich material from one leads to a thermonuclear runaway on a white-dwarf companion. Despite years of study, many open questions remain [2–4]: How much mass do novae eject? Do novae form grains that can be captured and analyzed on Earth? Is there a link between recurrent novae and type Ia supernovae? Additional observational constraints are needed to resolve these open issues.

A rather direct constraint on nova models could come from the observation of discrete-line γ rays from the decay of radioisotopes produced by the nucleosynthesis in novae. The most promising targets for observation are those radioactive isotopes produced in large amounts and with half-lives long enough to survive until the atmosphere is transparent to radiation. This γ-ray emission is thought to be dominated by the decay of ^{18}F during the first day or so after the initial outburst [5,6], and thus understanding the nuclear reactions affecting ^{18}F nucleosynthesis in novae is critical to interpretation of this γ-ray signature.

After production the largest loss of ^{18}F occurs via the $^{18}F(p,\alpha)^{15}O$ reaction, and several studies have identified this reaction as one of the 3 most important for novae for further experimental investigations [7,8]. A variety of direct [9–13] and indirect measurements with both stable [14–16] and radioactive beams [17–19] have been used to characterize the reaction rate [20]. The primary temperature range for novae nucleosynthesis is 0.05–0.40 GK, and the rate is dominated towards the higher end of this range by contributions through a $\frac{3}{2}^+$ resonance at $E_{c.m.} = 665$ keV [10] and a $\frac{3}{2}^-$ resonance at $E_{c.m.} = 330$ keV [11] above the proton threshold at 6.4100(5) MeV in ^{19}Ne. At the lower

* Corresponding author at: Dept. of Physics, University of Notre Dame, Notre Dame, IN 46556, USA.
E-mail address: danbardayan@nd.edu (D.W. Bardayan).

http://dx.doi.org/10.1016/j.physletb.2015.10.073

end of the temperature range, the rate is far more uncertain because of the unknown properties of near-threshold levels and the possible interference between these and higher-lying broad resonances. Guidance has also come from a recent theoretical study, which pointed to the importance of previously neglected s-wave $\frac{1}{2}^+$ resonances [21]. This study predicted that a broad $\frac{1}{2}^+$ level above $E_{c.m.} = 1$ MeV would interfere with a subthreshold $\frac{1}{2}^+$ resonance to reduce the importance of $\frac{3}{2}^+$ resonance contributions upon which most previous estimates of the rate were based.

Spurred in part by these predictions and the need to pinpoint which resonances had significant (p,α) strength, a proton-transfer study was performed that preferentially populated states of importance to the ^{18}F$(p,\alpha)^{15}$O reaction [19]. While not all ^{19}Ne levels were expected to be observed, any level with significant single-particle strength would be populated. That study found tantalizing evidence of a strong subthreshold level at $E_{c.m.} = -122$ keV that was populated with an angular momentum transfer consistent with a $\frac{1}{2}^+$ assignment. Unfortunately, it could not be determined whether the state was a $\frac{1}{2}^+$ or $\frac{3}{2}^+$ level, and thus significant uncertainty remained in the expected interference and reaction rate. In this letter, we report on the first science result using the Jet Experiments in Nuclear Structure and Astrophysics (JENSA) gas-jet target [22] to definitively determine the spin and nature of this strong subthreshold resonance.

This manuscript presents the first peer-reviewed study of the ^{20}Ne$(p,d)^{19}$Ne reaction. Deuterons populating the subthreshold state of interest at $E_x = 6288$ keV would exhibit angular distributions indicative of the spin of the level. In this study, a $\frac{1}{2}^+$ level or $\frac{3}{2}^+$ level would be populated with an $\ell = 0$ and 2 angular-momentum transfer, respectively, which in turn would produce significantly different angular distributions for the outgoing deuterons. The experiment utilized a 30-MeV proton beam from the Holifield Radioactive Ion Beam Facility [23] to bombard a gas jet of ^{nat}Ne ($\sim 91\%$ ^{20}Ne). Reaction deuterons were detected and identified using the SIDAR Silicon Detector Array [24] configured in telescope mode with 65-μm-thick detectors being backed by 1000-μm-thick detectors and covering laboratory angles between 18° and 53°. A previous attempt to study this reaction [25,26] had used a thin C target in which Ne had been implanted. It was found, however, that (p,d) reactions on the other components in the target besides Ne presented too much background from which to separate the ^{20}Ne$(p,d)^{19}$Ne events of interest. A localized and pure Ne gas target was needed, and thus the JENSA gas-jet target was well-suited for this application.

A full description of the JENSA gas-jet target is given in Ref. [22]. Briefly, high pressure gas ($\sim 16\,000$ Torr) is injected through a Laval nozzle to form a dense jet of gas approximately 4 mm wide. After passing through the target region, the gas is received, compressed, and recirculated back through the target with the aid of multiple stages of pumping and compression. The interaction point of the beam with the gas jet is surrounded by arrays of silicon detectors such as SIDAR, the Oak Ridge Rutgers University Barrel Array (ORRUBA) [27], and SuperORRUBA [28]. The effective areal density of the jet was estimated by measuring the energy loss of α particles emitted from a ^{244}Cm source and was found to be $\sim 4 \times 10^{18}$ Ne atoms/cm^2. Precise knowledge of this areal density was not needed for this experiment, however, since the angular distribution of deuterons was measured at all angles simultaneously.

The observed deuteron spectrum produced at 29° after bombardment with 3 nA proton beams for 15 hours is shown in Fig. 1. The spectrum shows excellent correspondence with known ^{19}Ne levels. As opposed to the previous attempts [25,26], there was no observable elemental contamination of the target. A few deuteron peaks were observed from the ^{22}Ne$(p,d)^{21}$Ne reaction (labeled as ^{22}Ne in Fig. 1), but those were easily identified by their differing kinematic curves. All other peaks correspond to known states in ^{19}Ne. The relatively smooth background between the peaks in the spectrum arises from effects such as incomplete charge collection in the silicon detectors and random coincidences in the deuteron gate arising primarily from pileup of elastically-scattered proton pulses. The deuteron energy calibration was performed using the strongly populated, isolated, and well-known levels at $E_x = 0$, 2795, and 6742 keV. The excitation energies reflecting the average from all of the angles in this work are compared with those from the compilation [29] in Table 1. The uncertainties quoted in the present results are purely statistical in nature. From comparison of the extracted excitation energies with the calibration peaks, we estimate the systematic uncertainties to be on the order of ±3 keV.

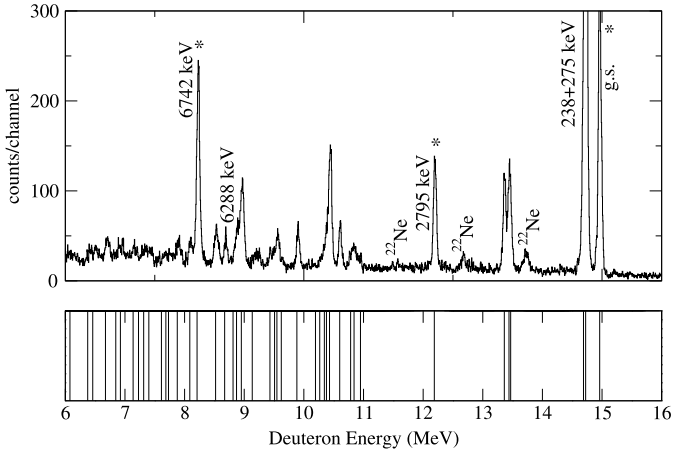

Fig. 1. The top panel shows the observed deuteron energy spectrum at 29° while the bottom panel shows the expected energies for the population of known levels in the ^{20}Ne$(p,d)^{19}$Ne reaction at the same angle and a bombarding energy of 30 MeV. Peaks labeled with stars were used for energy calibration.

Table 1
The ^{19}Ne excitation energies in keV from this work are compared with those from the most recent evaluation [29] and those from Laird et al. [16]. The states marked with an asterisk were used for the internal energy calibration. Only statistical uncertainties are quoted. There is an additional ± 2 keV systematic uncertainty in the energies from Ref. [16] and an additional ±3 keV systematic uncertainty in the present results.

Compilation	Present work	Laird et al.
0*	2(2)	
238.27(11) + 275.09(13)	255(2)	
1507.56(30) + 1536.0(4)	1524(2)	
1615.6(5)	1604(3)	
2794.7(6)*	2792(3)	
4032.9(24)	4035(4)	
4140(4)	4153(4)	
4379.1(22)	4371(3)	
4549(4)	4556(3)	
5092(6)	5090(6)	
5424(7)	5424(7)	
5539(9)	5529(10)	
6013(7)	6017(3)	6014(2)
6092(8)	6101(4)	6097(3)
6288(7)	6282(3)	6289(3)
6437(9)	6438(2)	6440(3)
6742(7)*	6742(3)	6742(2)
6861(7)	6865(3)	6862(2)
7067(9)	7067(2)	

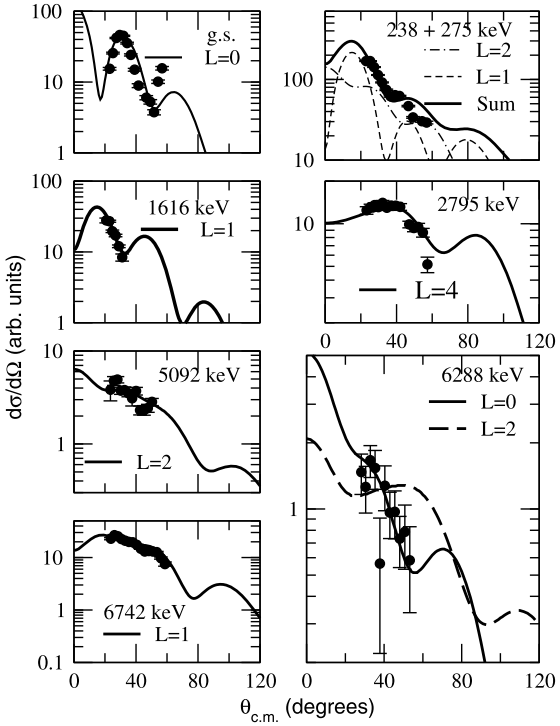

Fig. 2. Extracted angular distributions for the ^{20}Ne$(p,d)^{19}$Ne reaction. The distributions are compared to DWBA calculations using global optical model parameter sets.

The subthreshold state of interest was populated and identified at 6282 ± 3 keV, which is in agreement with the previous compilation and with the value reported by Adekola et al. [19].

The relative angular distributions of strongly-populated levels were extracted from the observed number of counts in each peak after background subtraction and using the known detector geometry. An absolute calibration of the normalized cross section was not possible since the beam current was not measured, but this did not compromise the goals of the experiment since determination of the transferred angular momentum is possible from extraction of the shape (i.e., the angular dependence) of the angular distribution. The measured angular distributions are plotted in Fig. 2. Gaps appear in the angular distributions where the peak of interest had too few counts above background, or for example in the case of the 1616-keV level, could not be resolved from a neighboring level at the outer angles where the kinematic broadening was more pronounced.

The experimentally-measured angular distributions were analyzed using finite range distorted-wave Born approximation (DWBA) calculations using the computer code TWOFNR7 [30]. Global optical model sets were used for the entrance and exit channels and provided a reasonable description of the observed angular distributions for well-known levels. For the initial state, the global potential parameters of Perey [31] were used, and in the exit channel, the potential parameters of Lohr and Haeberli [32] were used. It should be noted that the calculated angular distributions were primarily sensitive to the transferred angular momentum as opposed to the specific optical model parameters chosen. As can be seen in Fig. 2, the expected angular distributions agree well with those observed for levels with well-established spins [i.e., the excitation energies(spins) are known to be 0 keV ($\frac{1}{2}^+$), 238 keV ($\frac{5}{2}^+$), 275 keV ($\frac{1}{2}^-$), 1616 keV ($\frac{3}{2}^-$), 2795 keV ($\frac{9}{2}^+$), 5092 keV ($\frac{5}{2}^+$), 6742 keV ($\frac{3}{2}^-$) [29]]. A good $\ell = 4$ fit to the 2795-keV $9/2^+$ angular distribution was obtained despite the relatively small occupation of the $g_{9/2}$ neutron shell in the ^{20}Ne ground state.

The angular distribution for the state of interest at $E_x = 6288$ keV is also shown in Fig. 2. The angular distribution is well reproduced by an $\ell = 0$ transfer (taking into account the Q-value for the state) but is inconsistent with an $\ell = 2$ angular distribution. This confirms that the strong subthreshold ^{18}F$(p,\alpha)^{15}$O resonance is a $\frac{1}{2}^+$ ^{19}Ne level and cannot be a $\frac{3}{2}^+$ level. While this is in disagreement with the conclusion by Laird et al. [16] that a higher spin is preferred, the present study has the advantages of involving a simpler reaction on a spin zero target that populated several well-known levels for which the angular distribution analysis could be confirmed.

To explore the impact of the measurement, the ^{18}F$(p,\alpha)^{15}$O reaction rate has been calculated with the R-matrix code AZURE2 [33,34]. Resonances that were included in the reaction rate calculation are listed in Table 2 and are briefly described. The energy of the subthreshold resonance is the weighted average of those in Table 1 and the spin is from the present work. The ANC and Γ_α (scaled from the mirror level) are taken from Adekola et al. [19]. The energy for the 6.417-MeV level is the weighted average from the measurement of Laird et al. [16] and the compilation by Nesaraja et al. [20]. The spin and spectroscopic factor from Adekola et al. were used to scale Γ_p for the 1-keV change in energy. The alpha width is taken as an upper limit of 0.5 keV due to the lack of observation of the mirror in reanalysis of ^{15}N$(\alpha,\alpha)^{15}$N data [37]. The energy of the broad level at 6.439 MeV is the weighted average from Table 1 but with properties scaled from Nesaraja et al. The level at 6.457 MeV is assumed to be $\frac{3}{2}^+$ with properties from Nesaraja et al. but with an upper limit on Γ_p scaled from Adekola et al. for the change in energy. The 1.3-keV Γ_α was scaled by Nesaraja et al. from the mirror level width extracted in Ref. [37]. While the energy of this level has recently been questioned by Laird et al., it is certain that there must be a $\frac{3}{2}^+$ resonance in this energy range from comparisons with the mirror, and the upper limit on the proton width extracted by Adekola et al. constrains its influence. The properties of the $\frac{5}{2}^+$ level at 6.699-MeV level are taken mostly from Nesaraja et al. with an updated excitation energy from the weighted average of Laird et al. and Nesaraja et al. The $\frac{3}{2}^-$ level at 6.742 MeV is well studied with the proton-width coming from Ref. [11], the spin from Visser et al. [15], and the alpha width has been scaled from the mirror level by Nesaraja et al. The properties of the 7.076-MeV level were measured in Ref. [10]. Finally, the broad $\frac{1}{2}^+$ level at 1.46 MeV has been reported by Mountford et al. [13], Adekola et al. [35], and Dalouzy et al. [36]. We adopt partial widths for this level from Mountford et al. but consider the other measurements in our reaction rate

Table 2
The resonance parameters used and varied in the calculation of the ^{18}F$(p,\alpha)^{15}$O rate and its associated uncertainties. The ANC is given for the subthreshold resonance while other resonances are tabulated with their proton widths. Quantities come from measurements except where explicitly noted in the footnotes.

E_{res} (keV)	E_x (MeV)	$2J^\pi$	Γ_p (keV) or ANC (fm$^{1/2}$)	Γ_α (keV)
−124(3)	6.286(3)	1^+	83.5	11.6[a]
7(3)	6.417(3)	3^-	1.6×10^{-41}	< 0.5[a]
29(3)	6.439(3)	1^-	$< 3.8 \times 10^{-19}$[b]	220
47(3)	6.457(3)	3^+[a]	$< 2.1 \times 10^{-13}$	1.3[a]
289(3)	6.699(3)	5^+[a]	$< 2.4 \times 10^{-5}$[a]	1.2[a]
332(2)	6.742(2)	3^-	2.22×10^{-3}	5.2[a]
664.7(16)	7.0747(17)	3^+	15.2	23.8
1461(19)		1^+	55	347

[a] Adopted from mirror level.
[b] Based on assumed reduced proton width.

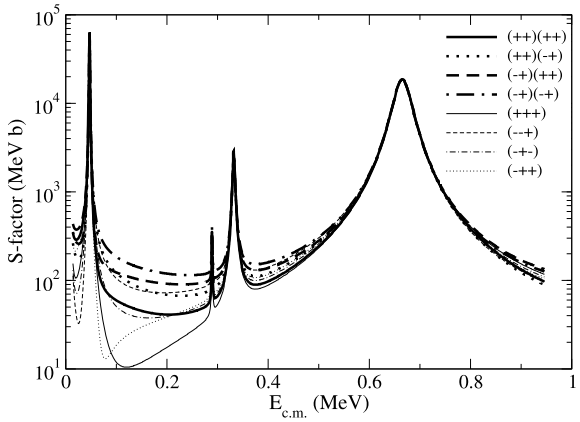

Fig. 3. Calculated ^{18}F$(p,\alpha)^{15}$O S-factors. Thick lines show the present values considering interference effects between $\frac{1}{2}^+$ and $\frac{3}{2}^+$ resonances. The notation is that the first pair in parenthesis designates the relative interference signs between $\frac{1}{2}^+$ resonances and the second pair designates the interference between $\frac{3}{2}^+$ resonances. The thin curves show the now excluded S-factors with a $\frac{3}{2}^+$ subthreshold resonance and interference between 3 resonances.

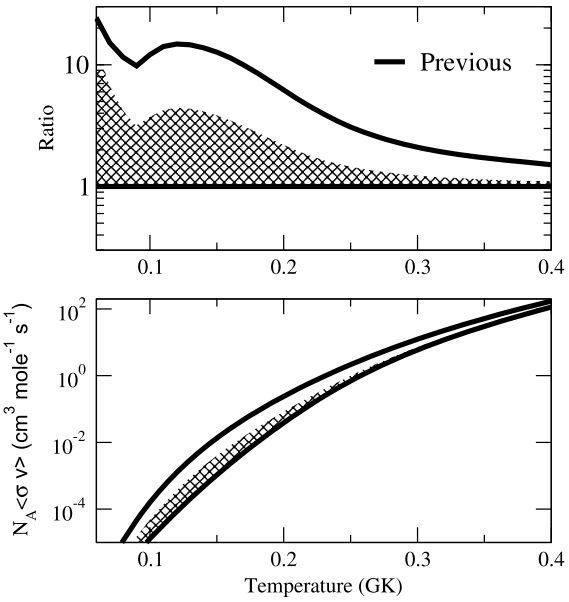

Fig. 4. The top panel shows the ratio of the ^{18}F$(p,\alpha)^{15}$O rate to the previously-calculated minimum rate [19] while the bottom panel shows the individual rates directly. The previous uncertainty band is outlined with solid lines, and the reduced uncertainty band from the current work is shown in white. The previous upper limit agrees with the current result, but the lower limit has been increased by a factor of 1.5–4.

calculations. No additional resonances have been considered because the ^{18}F$(d,n)^{19}$Ne measurements have shown there is very little single-particle strength outside of these known levels [19].

The astrophysical S-factor for the ^{18}F$(p,\alpha)^{15}$O reaction rate from the AZURE2 calculation is plotted in Fig. 3. As discussed in Ref. [19], the dominant uncertainty in the reaction rate results from the interference of subthreshold s-wave resonances with higher-lying broad resonances. Determination of the spin of the 6286-keV level greatly reduces uncertainties in these interference effects. Several uncertainties were considered to create the reaction rate uncertainty band in Fig. 4. First the reaction rate was calculated using the resonance parameters in Table 2. Quantities were then varied one at a time to gauge their influence on the calculated reaction rate. At each temperature, the low and high value of the resulting reaction rate calculations were tabulated to produce the plots in Fig. 4. Quantities considered were the signs of the interference, the energies of the resonances and the strengths that must be varied with the energies for certain resonances, and the considerable variations in the properties of the broad high-energy $\frac{1}{2}^+$ resonance. The deduced upper and lower limits on the rate are plotted in Fig. 4 with the current knowledge of the spin of the subthreshold resonance and are compared to the previous results. Since resonance parameters were varied within 1σ uncertainties, the reaction rate band can also be considered to be at the 1σ confidence level. It is found that the upper limit on the rate band remained the same, but the lower limit is increased by a factor of 1.5–4 over the temperature range 0.05–0.25 GK, which is in the primary temperature range for nova nucleosynthesis.

The implications have been investigated using the framework available through the Computational Infrastructure for Nuclear Astrophysics [38]. A "post-processing" approach was utilized following a reaction rate network through time profiles of temperature and density in 23 radial zones taken from one-dimensional hydrodynamic calculations of ONeMg nova outbursts on 1.15, 1.25, and 1.35 solar mass white dwarf stars [39]. A full reaction rate network was used in each zone with 169 isotopes from ^{1}H to ^{54}Cr. Reaction rates were taken from Reaclib [40] but varying the ^{18}F$(p,\alpha)^{15}$O rate within uncertainties. In all cases, it was found that the range of ejected ^{18}F mass has been reduced by about a factor of 2 owing to the reduction in uncertainty in the ^{18}F$(p,\alpha)^{15}$O rate. Since the ejected mass affects the distance at which ^{18}F can be detected (and thus the volume of space sampled with a given sensitivity), this results in a factor of 2.8 decrease in the uncertainty of detection probability owing to nuclear reaction rate uncertainties.

In summary, the astrophysical ^{18}F$(p,\alpha)^{15}$O reaction rate, and thus the nova nucleosynthesis of ^{18}F, has had significant uncertainties as a result of the uncertain properties of a strong subthreshold resonance. The uncertain interference between such a resonance and higher-energy broad s-wave resonances resulted in considerable variations in the estimated ^{18}F$(p,\alpha)^{15}$O reaction rate. A measurement with the new gas-jet target JENSA has been used to determine that the spin and parity of this subthreshold resonance is $\frac{1}{2}^+$, and this has significantly clarified the astrophysical ^{18}F$(p,\alpha)^{15}$O reaction rate. The remaining uncertainties are dominated by the lack of knowledge concerning a possible near-threshold $\frac{3}{2}^+$ level. Such a level exists in the mirror ^{19}F and the current upper limit on the resonance strength is not stringent enough to eliminate interference uncertainties. Further improvements in the reaction rate calculation could come from a better determination of the properties of levels near threshold [16], possibly from the study of decay γ-rays from these states or from measurements of the ^{18}F$(p,\alpha)^{15}$O cross section off resonance that could determine the nature of the interference. A simultaneous R-matrix fit of all available data sets could also improve our understanding of the rate. This first combination of modern large-area silicon detector arrays with supersonic gas-jet technology enables an entire program of research at existing and future radioactive beam facilities.

Acknowledgements

The authors gratefully acknowledge useful discussions with C. Brune, J. José, A. Laird, and H. Schatz. This work was supported by the National Science Foundation and the Department of Energy Office of Nuclear Physics. This work was also supported in part by the Joint Institute for Nuclear Astrophysics (JINA) under NSF Grant PHY 08-22648.

References

[1] S. Starrfield, et al., Astrophys. J. 176 (1972) 169.
[2] M.F. Bode, arXiv:1111.4941v1 [astro-ph].
[3] A. Parikh, et al., AIP Adv. 4 (2014) 041002.
[4] S. Starrfield, AIP Adv. 4 (2014) 041007.
[5] M. Hernanz, J. José, A. Coc, J. Gomez-Gomar, J. Isern, Astrophys. J. Lett. 526 (1999) L97.
[6] M. Hernanz, New Astron. Rev. 50 (2006) 504.
[7] J. José, J. Casanova, A. Parikh, E. García-Berro, J. Phys. G, Conf. Ser. 337 (2012) 012038.
[8] P.A. Denissenkov, et al., Mon. Not. R. Astron. Soc. 442 (2014) 2058.
[9] R. Coszach, et al., Phys. Lett. B 353 (1995) 184.
[10] D.W. Bardayan, et al., Phys. Rev. C 63 (2001) 065802.
[11] D.W. Bardayan, et al., Phys. Rev. Lett. 89 (2002) 262501.
[12] C.E. Beer, et al., Phys. Rev. C 83 (2011) 042801(R).
[13] D.J. Mountford, et al., Phys. Rev. C 85 (2012) 022801(R).
[14] S. Utku, et al., Phys. Rev. C 57 (1998) 2731.
[15] D.W. Visser, et al., Phys. Rev. C 69 (2004) 048801.
[16] A.M. Laird, et al., Phys. Rev. Lett. 110 (2013) 032502.
[17] N. de Séréville, et al., Phys. Rev. C 67 (2003) 052801.
[18] R.L. Kozub, et al., Phys. Rev. C 71 (2005) 032801(R).
[19] A.S. Adekola, et al., Phys. Rev. C 83 (2011) 052801(R).
[20] C.D. Nesaraja, et al., Phys. Rev. C 75 (2007) 055809.
[21] M. Dufour, P. Descouvemont, Nucl. Phys. A 785 (2007) 381.
[22] K.A. Chipps, et al., Nucl. Instrum. Methods Phys. Res., Sect. A 763 (2014) 553.
[23] J.R. Beene, et al., J. Phys. G, Nucl. Part. Phys. 38 (2011) 024002.
[24] D.W. Bardayan, et al., Phys. Rev. Lett. 83 (1999) 45.
[25] P.D. O'Malley, PhD thesis, Rutgers University, 2012.
[26] S.D. Pain, AIP Adv. 4 (2014) 041015.
[27] S.D. Pain, et al., Nucl. Instrum. Methods Phys. Res., Sect. B 261 (2007) 1122.
[28] D.W. Bardayan, et al., Nucl. Instrum. Methods Phys. Res., Sect. A 711 (2013) 160.
[29] D.R. Tilley, H.R. Weller, C.M. Cheves, R.M. Chasteler, Nucl. Phys. A 595 (1995) 1.
[30] J.A. Tostevin, private communication.
[31] C.M. Perey, F.G. Perey, At. Data Nucl. Data Tables 17 (1976) 1.
[32] J.M. Lohr, W. Haeberli, Nucl. Phys. A 381 (1974) 232.
[33] R.E. Azuma, et al., Phys. Rev. C 81 (2010) 045805.
[34] D.J. Mountford, et al., Nucl. Instrum. Methods Phys. Res., Sect. A 767 (2014) 359.
[35] A.S. Adekola, et al., Phys. Rev. C 85 (2012) 037601.
[36] J.C. Dalouzy, et al., Phys. Rev. Lett. 102 (2009) 162503.
[37] D.W. Bardayan, et al., Phys. Rev. C 71 (2005) 018801.
[38] http://nucastrodata.org.
[39] S. Starrfield, et al., Mon. Not. R. Astron. Soc. 296 (1998) 502.
[40] R.H. Cyburt, et al., Astrophys. J. Suppl. Ser. 189 (2010) 240.